

## Selective Interaction in a Polymer–Single-Wall Carbon Nanotube Composite

Marc in het Panhuis,<sup>\*,†</sup> Amitesh Maiti,<sup>‡</sup> Alan B. Dalton,<sup>§</sup> Albert van den Noort,<sup>†</sup>  
Jonathan N. Coleman,<sup>†</sup> Brendan McCarthy,<sup>†</sup> and Werner J. Blau<sup>†</sup>

Materials Ireland Polymer Research Centre, Department of Physics, Trinity College Dublin, Dublin 2, Ireland, Accelrys Inc., 9685 Scranton Road, San Diego, California 92121-3752, and NanoTech Institute, University of Texas at Dallas, Richardson, Texas 75080

Received: July 9, 2002; In Final Form: October 31, 2002

Purification and enhanced processability of carbon nanotubes have previously been achieved through interaction with a conjugated polymer. In particular, microscopy and Raman spectroscopy indicate a selective interaction between single-walled carbon nanotubes and a conjugated polymer. Until now, there has been no extensive theoretical investigation into the interaction between polymer and carbon nanotubes. An atomistic molecular dynamics computer simulation in conjunction with experimental evidence is used to elucidate the nature of the interaction. Computational time was reduced by representing carbon nanotubes as a force field. Our calculations indicate an extremely strong noncovalent binding energy. Furthermore, the correlation between the chirality of the nanotubes and mapping of the polymer onto the lattice is discussed.

## 1. Introduction

Carbon nanotubes (NT) can be employed in a wide variety of applications including space suit reinforcements, radar absorbance material for stealth applications, or as field emitters in display technology. This is due to their excellent structural, mechanical, and electronic properties. One of the main impediments to realizing applications is processing nanotubes. On the basis of their hydrophobic nature it was thought that NT would dissolve in a hydrophobic solvent such as toluene. However, carbon nanotubes fall out of toluene solution. It has been demonstrated that carbon nanotubes can be rendered soluble through noncovalent sidewall functionalization using poly(*m*-phenylenevinylene-*co*-2,5-dioctyloxy-*p*-phenylenevinylene) (PmPV) polymer<sup>1,2</sup> as a matrix.<sup>3,4</sup>

In the case of single-wall carbon nanotubes (SWNT), solubilization through sidewall functionalization has been achieved both by ourselves and other research groups.<sup>5–12</sup> In addition, functionalization has been used in the development of chemical sensors.<sup>13–15</sup> To preserve the SWNT electronic characteristics (i.e., the sp<sup>2</sup> hybridization), it is imperative to functionalize the sidewalls of SWNTs in noncovalent ways.

We have shown that PmPV entangles SWNT bundles into individual tubes.<sup>5</sup> Recently Bandyopadhyaya et al. have shown that Gum Arabic entangles SWNT ropes into individual, well-separated tubes.<sup>16</sup> Individual molecules such as  $\gamma$ -cyclodextrin can be used for debundling nanotubes.<sup>17</sup> Currently, the interaction between nanotubes and cyclodextrins is not well understood.

Recently Dai et al.<sup>18</sup> reported a simple and general approach for the noncovalent functionalization of the sidewalls of single-walled carbon nanotubes for immobilization of various biological molecules. In their approach, noncovalent functionalization was achieved using a bifunctional molecule, 1-pyrenebutanoic acid, succinimidyl ester.

Modeling work by other groups has shown the following. The Smalley group has investigated solubilization of SWNT in water with a linear polymer such as poly(vinyl pyrrolidone) and poly(styrene sulfonate),<sup>19</sup> and Lordi and Yao<sup>20</sup> performed energy minimization molecular mechanics calculations on PmPV. In addition, they calculated binding energies and frictional forces of functional groups and monomers.

Molecular dynamics simulations on carbon nanotubes have been conducted to investigate small molecules such as hydrogen and water inside nanotubes.<sup>21,22</sup> Recently, atomistic molecular dynamics simulations of carbon nanotubes in water were used to investigate structural characteristics and energetics.<sup>23</sup> Interaction between carbon nanotubes and water included an electrostatic interaction between carbon quadrupole moment and charge sites on water.

Our previous work<sup>11,12,24,25</sup> established the following optimal polymer characteristics for nanotube solubility. The PmPV polymer has a  $\pi$ -conjugated and twist allowing a backbone with solubilizing side groups. The PmPV backbone reorganizes into a relatively flat helical structure due to *m*-phenylene linkage and repulsive interactions between the octyloxy groups.<sup>12</sup> The exposure of the backbone plays an important role in facilitating (strong) induced dipolar binding between the polymer and the nanotube. The PmPV backbone can then easily  $\pi$  stack onto the nanotube. It is for this reason that PmPV with two octyloxy groups can hold nanotubes in solution, whereas PmPV with one octyloxy group<sup>26</sup> is not able to do this. In this geometry the polymer does not expose the backbone, while the octyloxy groups are projected outward under a 45° angle.<sup>12</sup> Of particular importance is the trans linkage in the repeat unit, which inhibits polymer aggregation. It was shown that an all-cis linkage could lead to entanglements between polymer side groups resulting in polymer aggregation, inhibiting interaction with the nanotubes. Without each of these components, PmPV-type polymers cannot be successful.<sup>11</sup> Our simulations in ref 12 did not reveal a helical structure for PmPV (in a vacuum) as reported by Lordi and Yao,<sup>20</sup> most likely due to the number of PmPV repeat units used in our calculations.

\* Author to whom correspondence should be address. E-mail: marc@panhuis.org.

<sup>†</sup> Trinity College.

<sup>‡</sup> Accelrys Inc.

<sup>§</sup> University of Texas.

It should be pointed out that the presence of a  $\pi$ -conjugated backbone is not crucial in holding nanotubes in solution as our work on poly(vinyl alcohol) PVA has shown.<sup>27</sup> However, we suggest that PVA holds a lower content of tubes in solution for two reasons. (i) The first is the absence of an exposed backbone with a large surface area such as observed for PmPV. Therefore, it is relatively easy for the PmPV backbone to  $\pi$  stack onto the tubes. (ii) Second, PVA has a lower permanent dipole moment, which results in a lower induced dipole moment in the tubes and a lower polymer nanotube binding energy.

In this paper, atomistic computer simulation and experimental observations are combined to identify the binding energy necessary to destroy nanotube bundles using PmPV polymer. Furthermore, the wrapping characteristics of PmPV onto single-walled nanotubes are investigated. A theoretical estimation of the attractive binding energy resulting from dipole–induced dipole interaction is presented. The results are compared to recent experimental observations and discussed accordingly.

## 2. Experimental Observations

In our experimental studies<sup>5,28</sup> it was found that as most polymer is mostly bound to the SWNT there is very little free polymer present. It is also evident that the SWNTs are well dispersed within the system. Good wetting between the SWNTs and the PmPV was observed. The SWNT appeared to have an ordered, cylindrically symmetric coating of the polymer.

When examining comparable samples by scanning tunneling microscopy (STM), similar structures can be observed.<sup>28</sup> This suggests mapping of the polymer onto the helical conformation of the nanotube.

In ref 28 it was suggested that the angle of the underlying wrapping must be indicative of the underlying symmetry, i.e., the chirality of the nanotube. For this particular system a band gap of 0.6 eV was obtained, suggesting a nanotube diameter of 1.28 nm, since the band gap is inversely proportional to the diameter.

In a previous optical study it has been shown that at low loading levels the polymer acts to de-bundle ropes, resulting in individually coated nanotubes.<sup>5</sup> These systems were extensively studied using Raman spectroscopy. Large modification to the well-known G-line feature in nanotubes indicated that the polymer intercalates between tubes, thus preventing them from re-aggregating after treatment. This was further strengthened by the observation that the radial breathing modes, whose frequency position is extremely sensitive to tube diameter and chirality,<sup>5</sup> are upshifted by 21  $\text{cm}^{-1}$  compared to 14  $\text{cm}^{-1}$  in the case of tube–tube interactions in bundles. Moreover, there are also large modifications to the frequency distribution of modes in this region of the spectrum. A resonance Raman study, using several excitation energies, strongly suggests that these modifications can be assigned to the polymer selectively interacting with nanotubes within a diameter range of 1.3 to 1.5 nm and weakly with tubes of smaller and higher diameters. Due to the nature of this interaction, above 2% loading the selection process disappears, as the polymer is no longer capable of preventing tube aggregation.

## 3. Computational Method

To reduce computational time, carbon nanotubes are represented by a force field. A number of assumptions were made, the nanotube is rigid and at a fixed position, and the interactions with other molecules are governed through a van der Waals potential. The force acting on other molecules is calculated by constructing a grid throughout the simulation box. The grid has

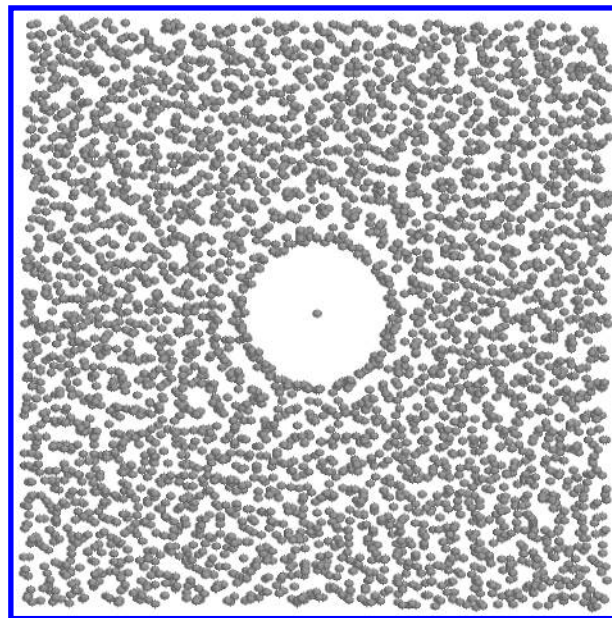


**Figure 1.** Snapshot of a carbon nanotube in a Lennard-Jones fluid.

to be constructed only once (at the beginning of a simulation) for each atom interacting with the carbon atoms of the nanotube. This procedure greatly reduces the demand for computational power.<sup>29</sup> The van der Waals parameters were taken from COMPASS force field.<sup>30</sup> The number of maxima refers to the number of aromatic rings in the nanotubes.

In section 2 it was found that chiral mapping was observed for SWNT with diameter 1.28 nm. Simulations were carried out on two SWNT (13,6) and (12,7) with diameter around 1.3 nm. Atomistic molecular dynamics simulations<sup>31</sup> were carried out using the COMPASS force field for (12,7) and (13,6) SWNT and 4 repeat units of PmPV (in a vacuum). The repeat unit used in our polymer/nanotube system is 10.2 Å, equaling 1 repeat unit of PmPV polymer. Using 4 polymer repeat units results in a wrapping of 40.8 Å of nanotube. The binding energy was extracted from the difference in the nanotube and polymer energy with the total energy,

$$E_{\text{binding}} = E_{\text{total}} - E_{\text{nanotube}} - E_{\text{polymer}}$$

## 4. Results and Discussion

The carbon nanotube force field was tested on a system with Lennard-Jones (LJ) particles at liquid density and room temperature. For practical reasons the LJ particles were given the same interaction parameters as the carbon atoms used in the SWNT force field. A snapshot of the simulation is shown in Figure 1. The gray dot in the middle indicates the center of a SWNT. The first and second solvation shells are clearly visible. The radial distribution function (RDF) between LJ particles and radial axis of SWNT indicates a third solvation shell (see Figure 2). The RDF has the shape that would be expected at liquid densities. The first solvation shell is found at 8.2 Å from the center of the SWNT. The RDF is in fact distorted and the peaks are lower than expected. The RDF was produced using a row of noninteracting sites along the axial direction of the SWNT. Subsequently the RDF was constructed using spherical volume elements, which produces the distorted curve. However, despite the distorted RDF the simulation clearly shows that the force field was implemented properly.

Binding energy calculations were performed on a close-packed arrangement of nanotube bundles (cell dimensions 16.0 Å  $\times$  16.0 Å,  $\gamma = 120^\circ$ , nanotube diameter 1.3 nm). The energy

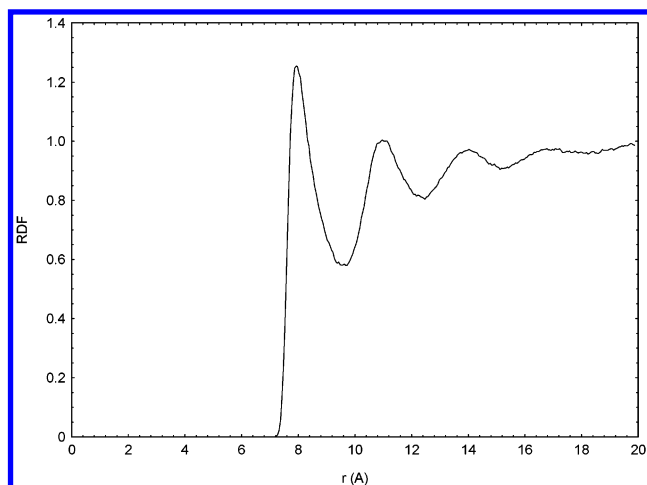


**Figure 2.** Radial distribution function (RDF) between a LJ particle and the radial axis of a SWNT.

**TABLE 1: Comparison of van der Waals Binding Energy between SWNT Bundle and PmPV Binding to Single SWNT (Diameter of SWNT is 1.3 nm; the repeat unit is 10.2 Å equal to one polymer repeat unit.)**

system	binding energy (kJ/mol per repeat unit)
SWNT in bundle (COMPASS)	479
PmPV-SWNT	159
PmPV backbone-SWNT	123
side chain (C <sub>8</sub> H <sub>17</sub> )-SWNT	36

gain from close packing per nanotube repeat unit (25.1 Å) is 479 kJ/mol (using COMPASS force field), roughly equivalent to 5 eV. The Goddard force field<sup>32</sup> is more accurate than COMPASS in estimating the van der Waals interaction between graphite planes. The elastic properties of graphite are reproduced very well using the Goddard force field. The cohesive energy for a nanotubes bundle was found to be 333 kJ/mol per repeat unit. The optimized isolated structure of PmPV using the COMPASS force field was found to be in good agreement with the previous reported structure.<sup>12</sup>

The simulations showed that the PmPV conformation changes from its minimum energy configuration due to interactions with nanotubes as shown in Figure 3A,B.

Table 1 shows the binding energy contributions of the polymer backbone and side chain to the total binding energy. The total binding energy per (polymer) repeat unit is 159 kJ/mol. The polymer backbone provides a binding energy of 123 kJ/mol per repeat unit. Alternating side-chains bind to the tube. Therefore, the binding energy for the side chains is 36 kJ/mol per repeat unit.

Thus, absorbance of 3 polymer strands can disperse an individual carbon nanotube (of equal length). From the PmPV/nanotube structure shown in Figure 3 it is certainly possible to place a second and maybe a third PmPV running parallel to the tube length. Each PmPV provides a 120° covering of the tube. Therefore, it is clear that a dense coverage by the polymer is necessary on the tube surface to effectively disperse the tubes. Simulations of interactions with graphite surface yielded no significant preference for alignment along the hexagon rows, both for polymer backbone and side-chain. Table 2 displays the binding energy for three angles of tilt (0°, 15°, and 30°) of the backbone to the tube axis. It was observed that the side-chain is very floppy and can deform itself easily on the nanotubes surface. However, the polymer backbone has a preference to be "straight". The preferred PmPV alignment onto the nanotubes backbone is shown in Figure 3C.

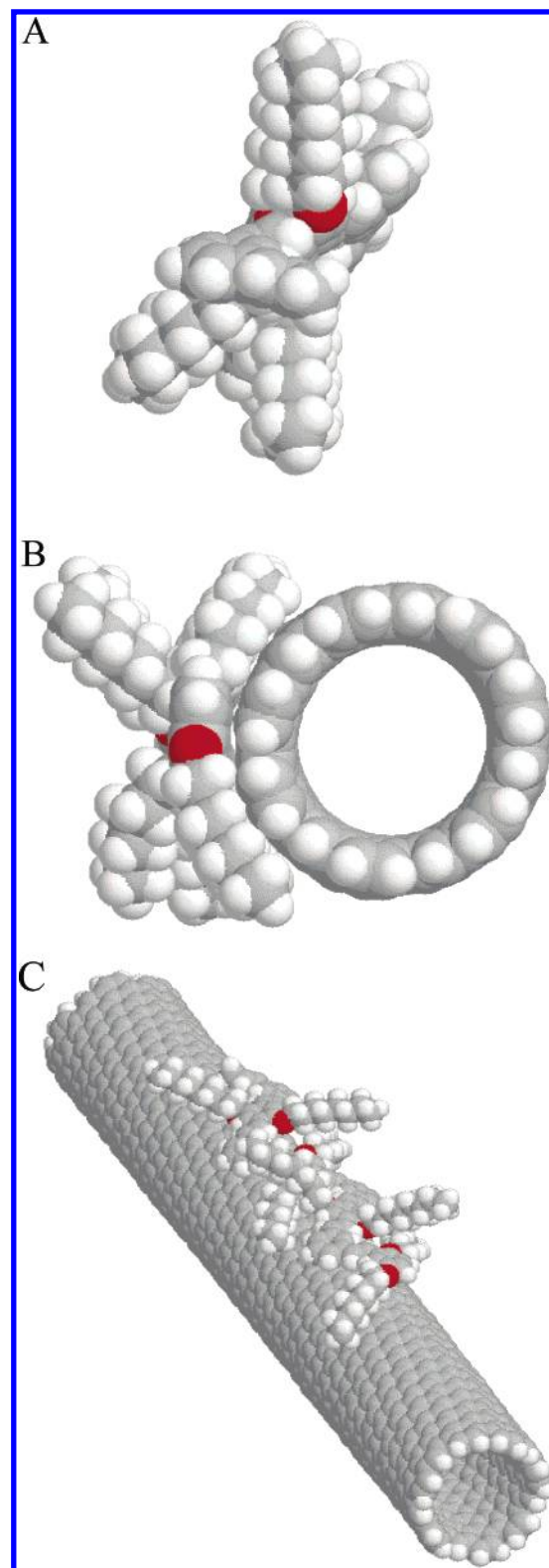


**Figure 3.** PmPV polymer (4 repeat units) wrapped onto a (12,7) carbon nanotube in a vacuum. (A) isolated polymer, (B) polymer on nanotube side view, and (C) top view. Carbon, hydrogen, and oxygen atoms are shown in gray, white, and red, respectively.

The results above imply that the lowest energy configuration would involve the polymer nanotube running along the tube axis, while side-chains of alternating phenyl rings adhere to the tube, although not necessarily along the row of hexagons.

Thus, the polymer is capable of preventing re-aggregation of SWNTs into bundles if the van der Waals (induced dipolar binding) forces are larger than the inter-nanotube forces in the



**TABLE 2: Van Der Waals Binding Energy as a Function of the Angle between Hexagons Rows of the Graphite Surface and the Backbone of the PmPV Polymer (The repeat unit is 10.2 Å equal to one polymer repeat unit.)**

backbone tilt angle to tube axis (degrees)	backbone binding energy (kJ/mol per repeat unit)
0	123
15	116
30	110

bundle. It is energetically more favorable for PmPV to self-assemble onto each individual SWNT than to coat the SWNT bundles. There is, however, an optimum for the formation of these PmPV self-assembled layers (SAL). We suggest that the selective interaction might be a result of packing density. For tubes with diameter between 1.3 and 1.5 nm, the polymer packing onto SWNTs is at its optimum. For smaller diameters, the polymer is not able to coat the SWNTs effectively. As a result these tubes are not held in solution. In our previous work it has been shown that PmPV can hold multiwall carbon nanotubes (diameter larger than 1.5 nm) in solution.<sup>3,4</sup> Therefore, it is suggested that instead of the packing density the solvent effects might exclude larger diameters SWNT.

An interesting question to address would be to determine what is the smallest diameter that can be dispersed from the bundles and the optimum length of the side chains used.

Let us now address the strength of the attractive interaction between carbon nanotubes and polymers. Electrostatic interactions between the highly delocalized electron system of nanotube and polymers are governed by induced forces due to the highest polymer electrostatic moment. Polymer local dipole moments induce dipole moments on the nanotube, resulting in an attractive binding energy. The resulting inductive attractive energy between a dipolar entity and polarizable medium can be calculated according to the following equation:<sup>33</sup>

$$E_{\text{ind}} = -\mu^2\alpha/(4\pi\epsilon_0)^2r^6$$

where  $\mu$  represents the polymer local dipole moment,  $\alpha$  the static polarizability,  $\epsilon_0$  the vacuum permittivity, and  $r$  the distance between the local dipole moment and the nanotube surface. Thus, it is possible to make a comparison between the induced dipolar attractive binding energy of PVA and PmPV and carbon nanotubes. Please note that this is as an additional calculation (independent of the molecular dynamics simulations) used to investigate components of the binding energy.

Static polarizability data has been calculated using ab initio methods for small (5,5) and (9,0) SWNT.<sup>34</sup> The static polarizability a (9,0) SWNT was estimated at 792 AU. It is expected that the static polarizability of a (12,7) SWNT is approximately equivalent to (9,0) SWNT as their respective diameters are in the same order of magnitude. Simulations of PmPV–SWNT have shown that every PmPV repeat unit binds to the nanotube surface. Whereas, preliminary PVA–SWNT simulations have indicated that on average approximately 3 out of 10 PVA repeat units bind to the nanotube surface.<sup>29</sup> 10 PVA repeat units are approximately equal to 2 PmPV repeat units. This has to be taken into account when calculating the attractive energy. The polymer local dipole moments were estimated at approximately 4.16 D (PmPV) and 2.06 D (PVA) using Gaussian.<sup>35</sup> Self-consistent field calculations at the Hartree–Fock level lie within 15% of experiment.<sup>36</sup> The distance  $r$  is taken equal to the van der Waals distance of 3.36 Å. The attractive energy between SWNT–PmPV is estimated at 84.8 kJ/mol per NT repeat unit,

whereas the SWNT–PVA attractive energy is estimated at 21.0 kJ/mol per NT repeat unit. This confirms that both conformational and electrostatic aspects play an important role in facilitating polymer binding to nanotubes. The presence of the conjugated backbone in PmPV allows all local dipole moments to interact with the nanotube surface, whereas in the nonconjugated PVA only a fraction interacts with the nanotube. In addition, the stronger (calculated) local dipole moments result in stronger attractive energy.

Please note that this is just dipole–induced dipole attractive energy. The smaller attractive energy due between temporal dipoles in the polymer backbone and nanotube surface were not taken into account.

## 5. Conclusions

In conclusion, we have shown that the polymer conformation is altered from its lowest energy configuration due to interaction with the nanotube. Therefore, it is likely that the nanotubes are not inside a polymer coil (as observed in a solvent) as was tentatively suggested by us.<sup>3</sup> Instead, the polymer alters its coil (as observed in a solvent) configuration in order to wrap (around) the nanotube in an ordered fashion as observed in ref 28.

Simulation suggests that the polymer backbone provides the strongest binding (123 kJ/mol per PmPV repeat unit) to the nanotubes and not the side groups. The binding energy of the octoloxo side chains is significantly lower (36 kJ/mol per PmPV repeat unit). Thus, the side chains have a much greater freedom of movement. In addition, our calculations show that it is energetically more favorable for the polymer to lie along the parallel axis instead of mapping onto the chirality of the underlying tube. Therefore with this level of computer simulation, we are not able to confirm the chiral polymer mapping suggested from STM studies.<sup>28</sup> The observed mapping might be a result of the greater degree of freedom of the side chains and polymer–polymer interactions between multiple polymer strands.

To explain the selective interaction we suggest the following. SWNT are produced in bundles. For simplicity it is assumed that the nanotubes have a uniform nanotube diameter. During sonication PmPV self-assembles onto the nanotubes, thereby preventing nanotube reaggregation. Our calculations have shown that the attractive (polymer)–(SWNT) induced dipole forces are stronger than the inter-tubular forces. However, although each individual nanotube is coated, it is not always a perfect polymer packing as this depends on the tube diameter. Therefore, the repulsive forces between SWNT and solvent can cause nanotubes to fall out of solution. If the packing density of the SAL is near perfect, i.e., full shielding of the nanotubes from the repulsive solvent forces, the nanotubes will remain in solution.

It has been shown that the attractive binding energy between polymer and nanotube can be estimated using the nanotube polarizability and local polymer dipole moments. It has been calculated that due to conformational differences in the polymer backbone PmPV binds significantly more strongly to the nanotube compared to PVA. This simple method combining polymer conformation, nanotube polarizability, and polymer local dipole moment allows us to make a quantitative comparison between the attractive binding energy.

The self-assembly properties of molecules such as polymers and proteins can be used to alter the electronic properties of SWNT/MWNT to be used for example as sensing electrodes in nanoscale sensors.<sup>13–15</sup>

**Acknowledgment.** M.ihP., A.vdN., J.N.C., B.M.C., and W.J.B. thank the Irish Higher Education Authority (HEA) and EU Network Programs Nanocomp and Comelcan for financial assistance. A.B.D. gratefully acknowledges financial support from DARPA. A.vdN. thanks Stichting Universiteitsfonds Twente. M.ihP. and A.vdN. thank W. J. Briels for useful discussions.

## References and Notes

- Holzer, W.; Penzkofer, A.; Gong, S. H.; Bleyer, A.; Bradley, D. C. *Adv. Mater.* **1996**, *8*, 974.
- Davey, A. P.; Drury, A.; Maier, S.; Byrne, H. J.; Blau, W. J. *Synth. Met.* **1999**, *103*, 2478.
- Curran, S. A.; Ajayan, P. M.; Blau, W. J.; Carroll, D. L.; Coleman, J. N.; Dalton, A. B.; Davey, A. P.; Drury, A.; McCarthy, B.; Maier, S.; Strevens, A. *Adv. Mater.* **1998**, *10*, 1091.
- Coleman, J. N.; Dalton, A. B.; Curran, S.; Rubio, A.; Davey, A. P.; Drury, A.; McCarthy, B.; Lahr, B.; Ajayan, P. M.; Roth, S.; Barklie, R. C.; Blau, W. J. *Adv. Mater.* **2000**, *12*, 213.
- Dalton, A. B.; Stephan, C.; Coleman, J. N.; McCarthy, B.; Ajayan, P. M.; Lefrant, S.; Bernier, P.; Blau, W. J.; Byrne, H. J. *J. Phys. Chem. B* **2000**, *104*, 10012.
- Dalton, A. B.; Blau, W. J.; Chambers, G.; Coleman, J. N.; Henderson, K.; Lefrant, S.; McCarthy, B.; Stephan, C.; Byrne, H. J. *Synth. Met.* **2001**, *121*, 1217.
- McCarthy, B.; Coleman, J. N.; Curran, S. A.; Dalton, A. B.; Davey, A. P.; Konya, Z.; Fonseca, A.; Nagy, J. B.; Blau, W. J. *J. Mater. Sci. Lett.* **2000**, *19*, 2239.
- Liu, J.; Rinzler, A. G.; Dai, H.; Hafner, J. H.; Bradley, R. K.; Boul, P. J.; Lu, A.; Iverson, T.; Shelimov, K.; Huffman, C. B.; Rodriguez-Macias, F.; Shon, Y.-S.; Lee, T. R.; Colbert, D. T.; Smalley, R. E. *Science* **1998**, *280*, 1253.
- Chen, J.; Hammon, M. A.; Hu, H.; Chen, Y. S.; Rao, A. M.; Eklund, P. C.; Haddon, R. C. *Science* **1998**, *280*, 95.
- Boul, P.; Liu, J.; Mickelson, E.; Huffman, C.; Ericson, L.; Chiang, I.; Smith, K.; Colbert, D.; Hauge, R.; Margrave, J.; Smalley, R. E. *Chem. Phys. Lett.* **1999**, *310*, 367.
- Dalton, A. B.; Coleman, J. N.; in het Panhuis, M.; McCarthy, B.; Drury, A.; Blau, W. J.; Paci, B.; Nunzi, J.-M.; Byrne, H. J. *J. Photochem. Photobiol. A: Chem.* **2001**, *144*, 31.
- in het Panhuis, M.; Munn, R. W.; Blau, W. J. *Synth. Met.* **2001**, *121*, 1187.
- Kong, J.; Franklin, N.; Zhou, C.; Chapline, M.; Peng, S.; Cho, K.; Dai, H. *Science* **2000**, *287*, 622.
- Collins, P.; Bradley, K.; Ishigami, M.; Zettl, A. *Science* **2000**, *287*, 1801.
- Jhi, S.-H.; Louie, S. G.; Cohen, M. L. *Phys. Rev. Lett.* **2000**, *85*, 1710.
- Bandyopadhyaya, R.; Nativ-Rot, E.; Regev, O.; Yerushalmi Rozen, R.; *Nano Lett.* **2001**, *2*, 25.
- Chen, J.; Dyer, M. J.; Yu, M.-F. *J. Am. Chem. Soc.* **2001**, *123*, 6201.
- Chen, R. J.; Zhang, Y.; Wang, D.; Dai, H. *J. Am. Chem. Soc.* **2001**, *123*, 3838.
- O'Connell, M. J.; Boul, P.; Ericson, L. M.; Huffman, C.; Wang, Y.; Haroz, E.; Ausman, K. D.; Smalley, R. E. *Chem. Phys. Lett.* **2001**, *342*, 265.
- Lordi, V.; Yao, N. *J. Mater. Res.* **2000**, *15*, 2770.
- Froukakis, G. E. *Nano Lett.* **2001**, *1*, 172.
- Hummer, G.; Rasaiah, J. C.; Noworyta, J. P. *Nature* **2001**, *414*, 188.
- Walther, J. H.; Jaffe, R.; Halicioglu, T.; Koumoutsakos, P. *J. Phys. Chem. B* **2001**, *105*, 9980.
- Dalton, A. B.; Duesburg, G.; Coleman, J. N.; in het Panhuis, M.; Maiti, A.; McCarthy, B.; Blau, W. J.; Roth, S.; Byrne, H. J. *Recent Research Developments in Physical Chemistry*; Transworld Research Network, 2002; Vol. 6, 327.
- in het Panhuis, M.; Maiti, A.; Coleman, J. N.; Dalton, A. B.; McCarthy, B.; Blau, W. J. In *Electronic Properties of Molecular Nanostructures*; Kuzmany, H., Fink, J., Mehring, M., Roth, S., Eds.; *AIP Conf. Proc.* **2001**, *591*, 179.
- Drury, A.; Maier, S.; Davey, A. P.; Dalton, A. B.; Coleman, J. N.; Byrne, H. J.; Blau, W. J. *Synth. Met.* **2001**, *119*, 151.
- Cadek, M., et al. Unpublished results.
- McCarthy, B.; Coleman, J. N.; Czerw, R.; Dalton, A. B.; in het Panhuis, M.; Maiti, A.; Drury, A.; Byrne, H. J.; Carroll, D. L.; Blau, W. J. *J. Phys. Chem. B* **2002**, *106*, 2210.
- van den Noort, A. *Computer Simulations of Carbon Nanotubes and Polymers*; Project Report, Trinity College Dublin, 2001.
- Sun, H.; Rigby, D. *Spectrochim. Acta A* **1997**, *53*, 1301.
- Cerius 2 Software, Accelrys Inc, 9865 Scranton Road, San Diego, CA 92121-3752.
- Goddard, W. A., III; Karasawa, N. The MSXX force field for graphite: van der Waals parameters for Carbon. *J. Phys. Chem. B*, in press.
- Maitland, G. C.; Rigby, M.; Smith, E. B.; Wakeham, W. A. *Intermolecular forces: their origin and determination*; Clarendon Press: Oxford, 1981.
- Jensen, L.; Schmidt, O. H.; Mikkelsen, K. V.; Åstrand, P.-O. *J. Phys. Chem. B* **2000**, *104*, 10462.
- Frisch, M. J.; Trucks, G. W.; Schlegel, H. B., et al. *Gaussian 94* (Revision A.1); Gaussian Inc.: Pittsburgh, PA, 1995.
- in het Panhuis, M.; Popelier, P. L. A.; Munn, R. W.; Ángyán, J. G. *J. Chem. Phys.* **2001**, *114*, 7951.